JOURNAL OF SYNCHROTRON RADIATION

Volume 28 (2021)

Supporting information for article:

Synchrotron Radiation X-ray Microtomography for the Visualization of Intra-Cochlear Anatomy in Human Temporal Bones Implanted with a Perimodiolar Cochlear Implant Electrode Array

Fergio Sismono, Lucia Mancini, Marc Leblans, Jana Goyens, Glynnis De Greve, Sara Schneiders, Karen Beckers, Joris Dirckx, Bert De Foer and Andrzej Zarowski

Here, we report some examples of images obtained by phase-contrast synchrotron-based computed microtomography reconstructed without and after the application of the single-distance phase retrieval Paganin's algorithm (Paganin et al., 2002) to the projection images prior to the reconstruction procedure. All tomographic slices have been reconstructed by using the STP software suite (Brun et al., 2015) and, after conversion to 16-bit tiff format, have been visualized through the Fiji software (Schindelin et al., 2012).

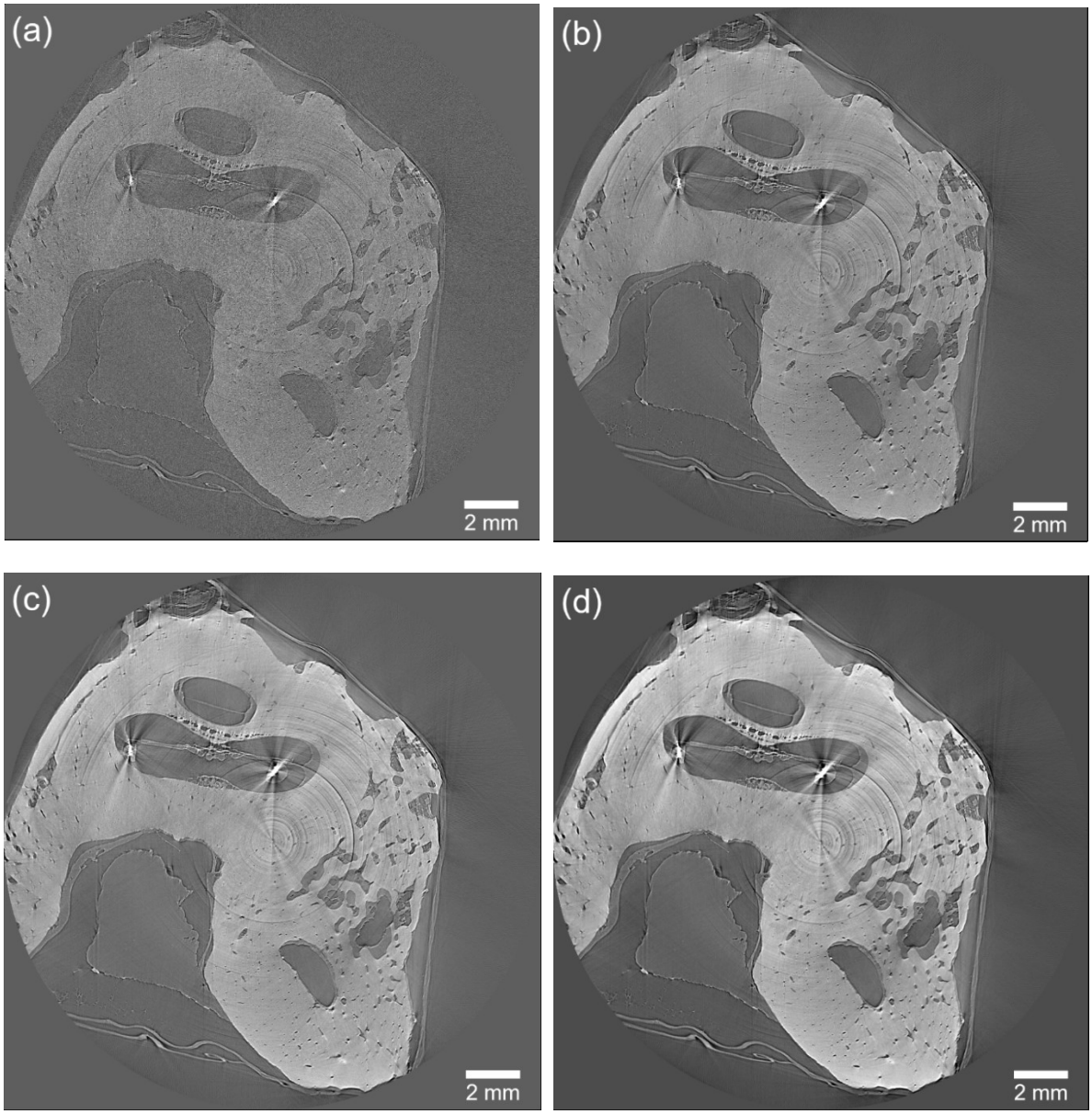

Figure S1 An axial slice of sample B09 reconstructed without (a) and after phase-retrieval with Paganin's algorithm at $\gamma = 100$ (b), $\gamma = 200$ (c) and $\gamma = 400$ (d).

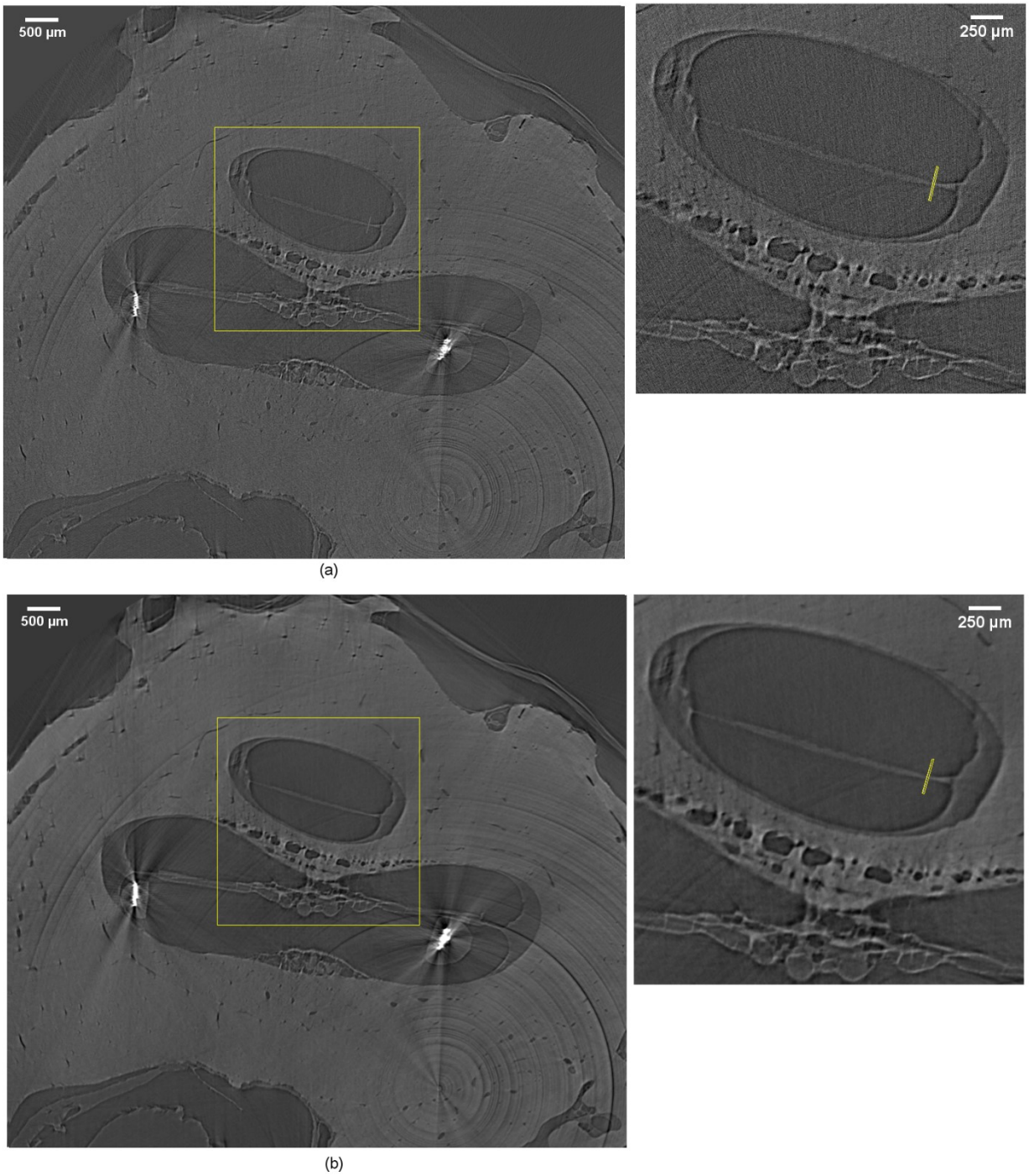

Figure S2 Crop of the axial slice of sample B09 showed in Figure S1 reconstructed without (a) and after (b) phase-retrieval (Paganin's algorithm, $\gamma = 200$). For each figure, an enlarged view in the region indicated by the yellow rectangle is reported. The inset yellow lines indicate the transects depicted in Fig. S3.

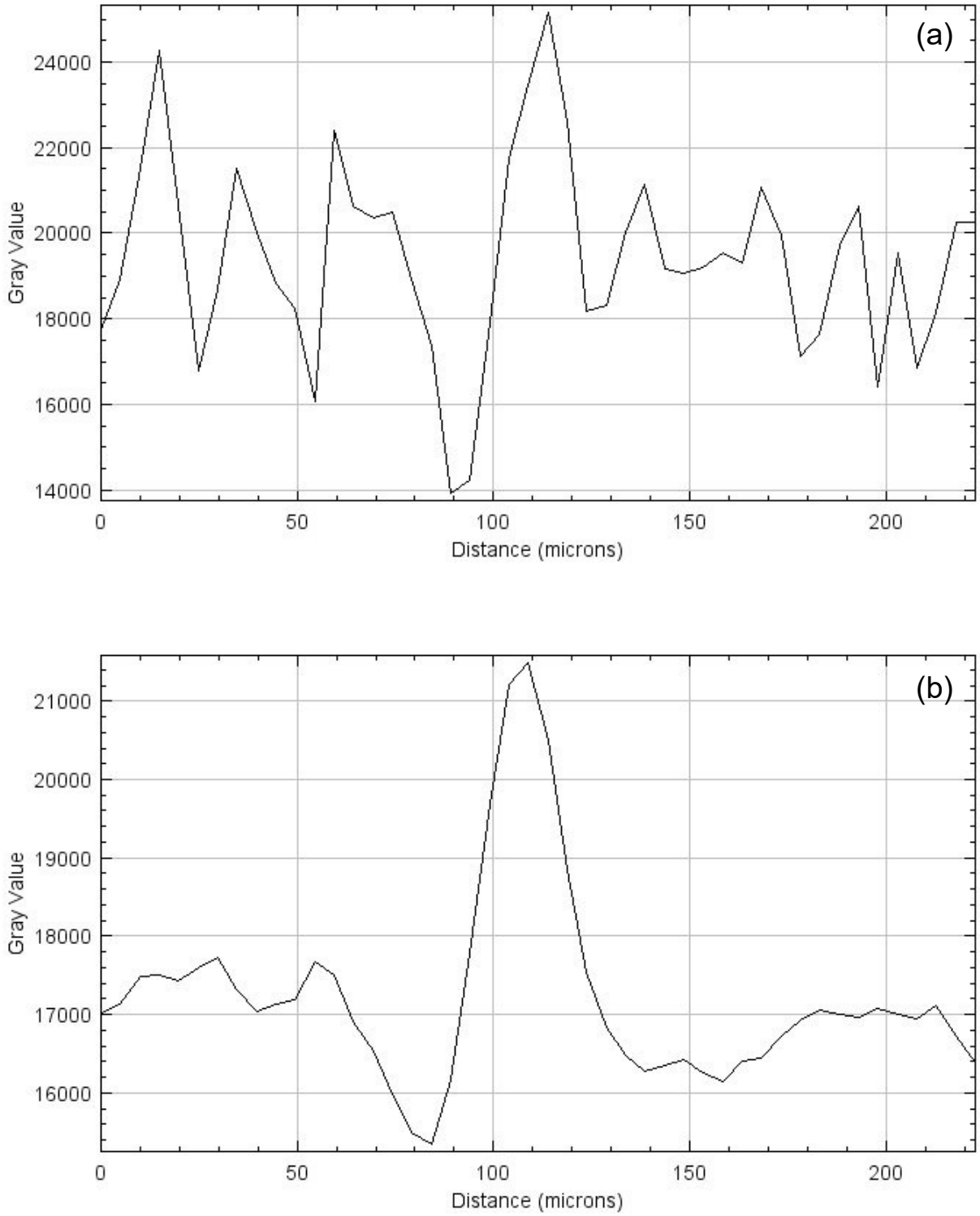

Figure S3 Grey-scale values along the transect depicted by yellow lines on Fig. S2. The membrane is much better distinguishable after (b), compared to without phase-retrieval (a), while the peak width remained comparable.

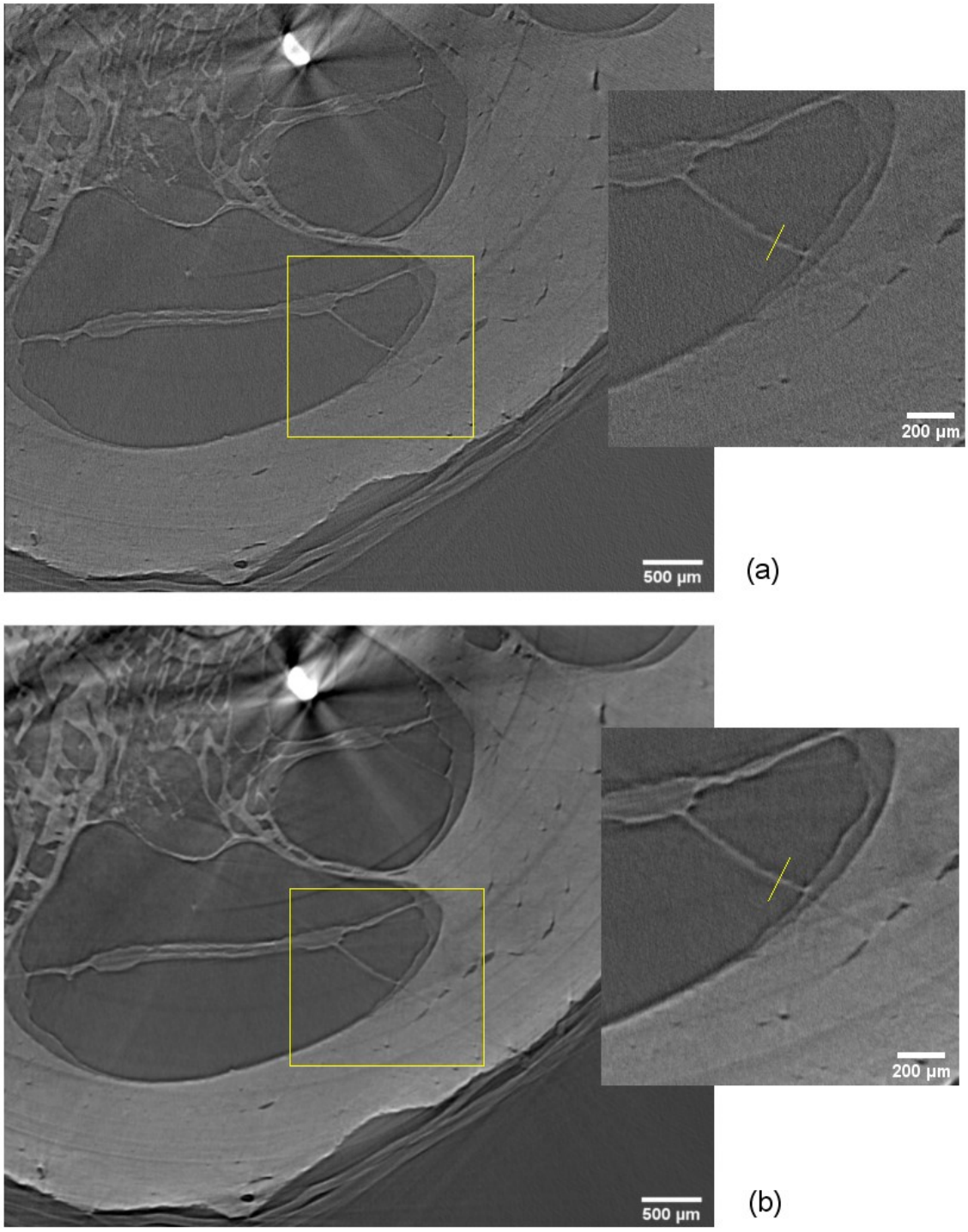

Figure S4 Crop of an axial slice of sample B07 reconstructed without (a) and after (b) phase-retrieval (Paganin's algorithm, $\gamma = 200$). For each figure, an enlarged view in the region indicated by the yellow rectangle is reported. The inset yellow lines indicate the transects depicted in Fig. S5.

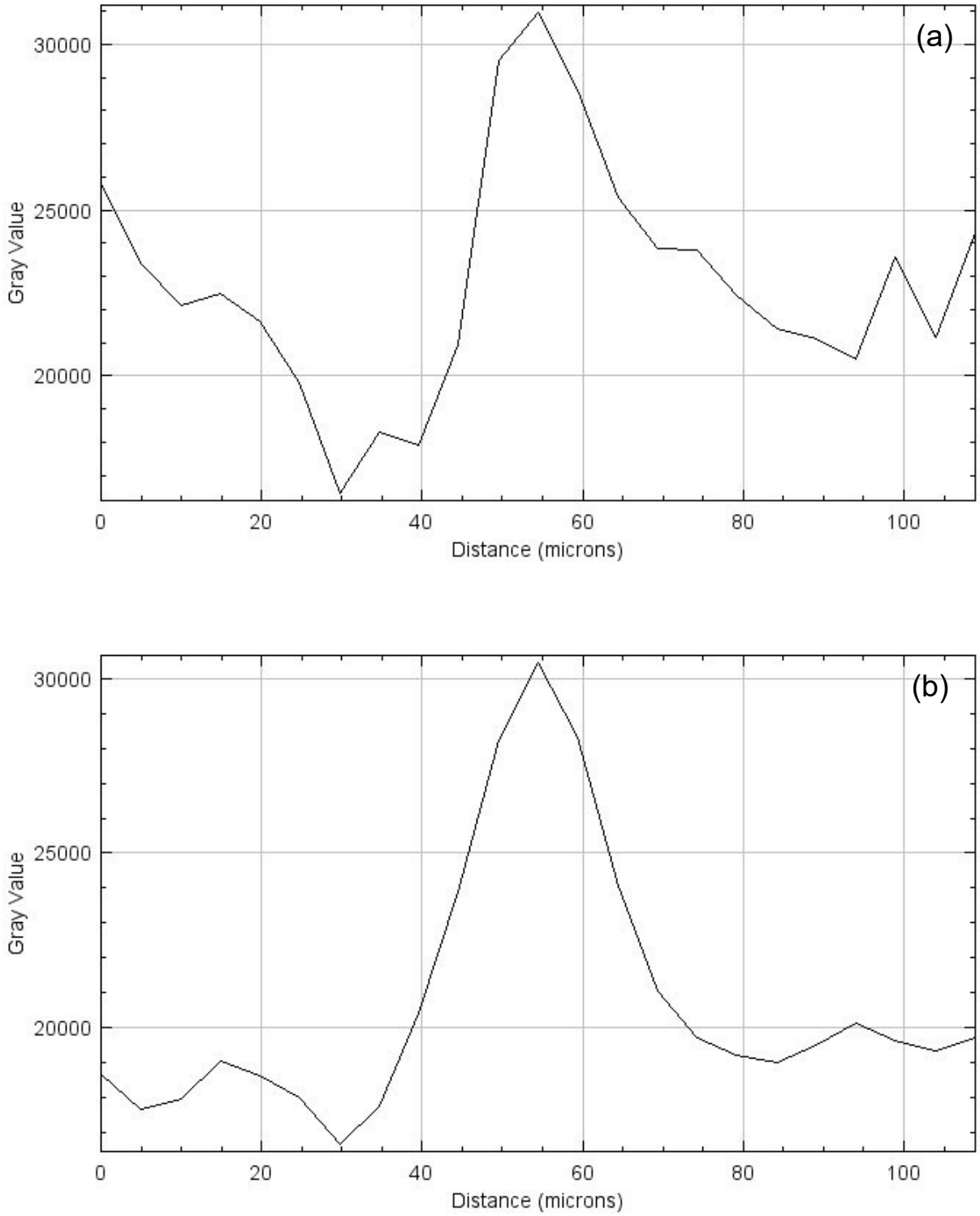

Figure S5 Grey-scale values along the transect depicted by yellow lines on Fig. S4. The membrane is much better distinguishable after (b), compared to without phase-retrieval (a), while the peak width remained comparable.

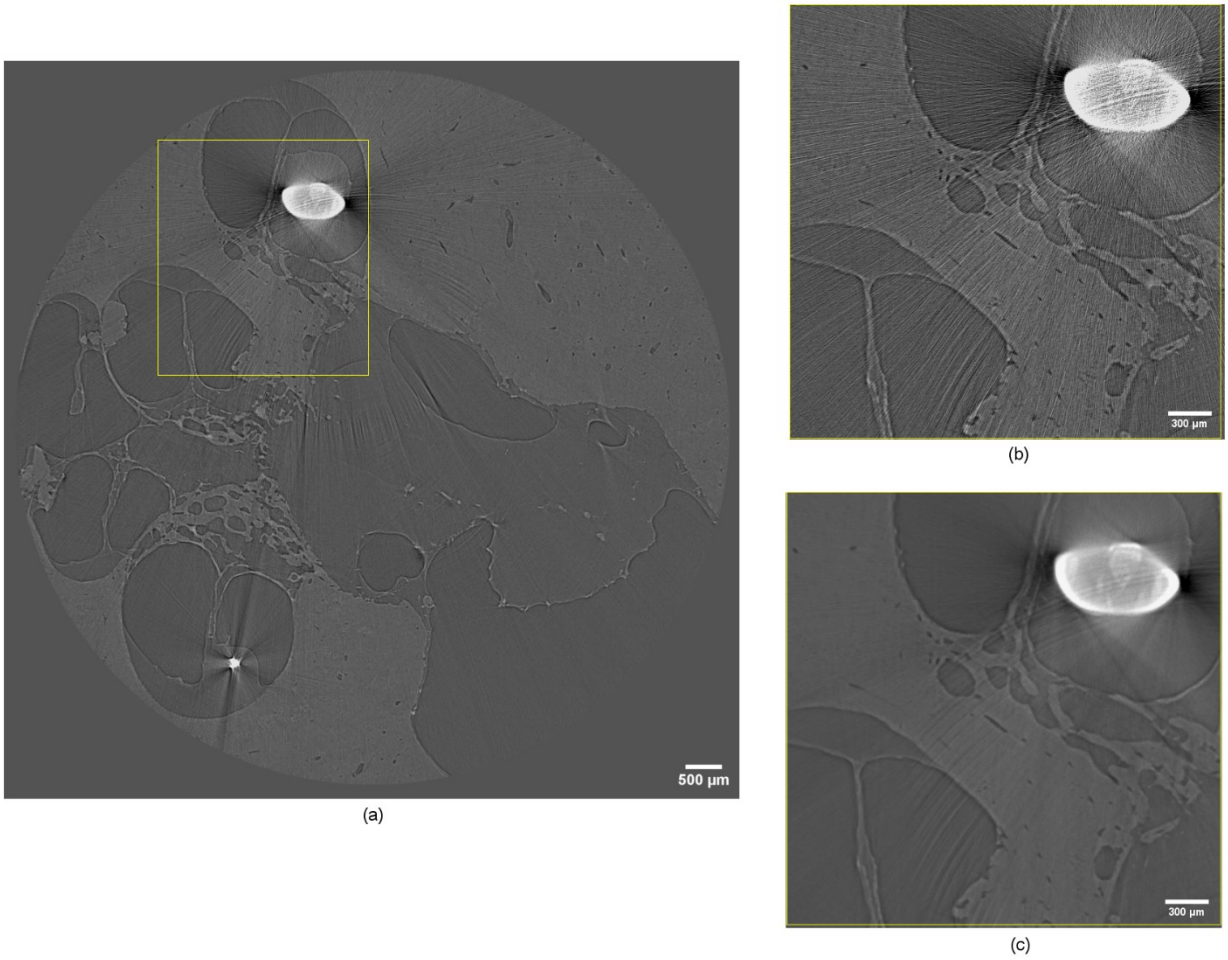

Figure S6 (a) A tomographic axial slice of sample A03 reconstructed without phase-retrieval. In (b) and (c) an enlarged view of the region indicated by the yellow rectangle is reported without and after phase-retrieval (Paganin's algorithm, $\gamma = 200$), respectively.

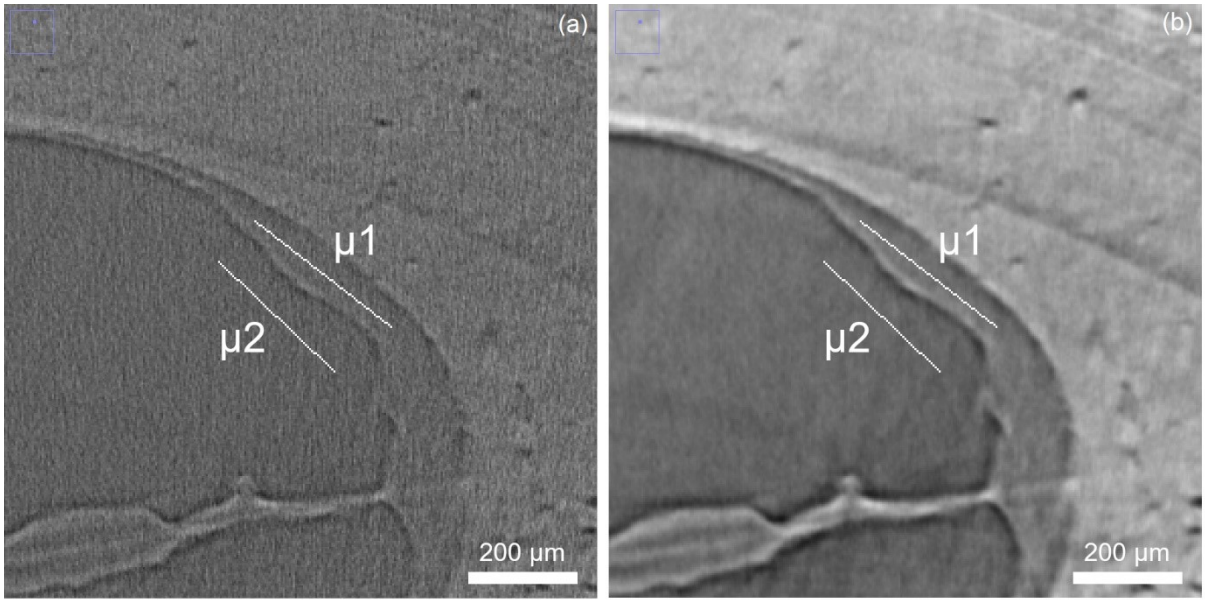

Figure S7 An axial slice crop of sample B07 without (a) and after (b) phase-retrieval (Paganin algorithm, $\gamma = 200$). The membrane contrast was evaluated by computing the contrast-to-noise ratio (CNR) (Goyens et al. 2018). $CNR = \frac{|\mu_1 - \mu_2|}{\sqrt{\frac{1}{2}(\sigma_1^2 + \sigma_2^2)}}$, where μ_1 and μ_2 are the mean grey-scale pixel values along transect lines across a section of membranous tissue (stria vascularis) and across a section of the air-filled cochlear duct, respectively. The CNR before phase-retrieval was equal to 0.49. After application of the phase-retrieval algorithm, the CNR increased roughly five-fold to a value of 2.63.

Movie S1 Animation showing the three-dimensional rendering of the sub-volume of sample B07 reported in Fig.2(b) of the main text.

References

Brun, F, Pacilè, S, Accardo, A,, Kourousias, G,, Dreossi, D., Mancini, L., Tromba, G., Pugliese, R. (2015). *Fund. Inform.* **141**, 233-243.

De Chaumont, F., Dallongeville, S., Chenouard, N., Hervé, N., Pop, S., Provoost, T., Meas-Yedid, V., Pankajakshan, P., Lecomte, T., Le Montagner, Y., Lagache, T., Dufour, A. & Olivo-Marin, J. C. (2012). *Nat. Methods*. **9**, 690–696.

Goyens, J., Vasilopoulou-Kampitsi, M., Claes, R., Sijbers, J. & Mancini, L. (2018). *J. Anat.* **233**, 770–782.

Paganin, D., Mayo, S.C., Gureyev, T.E., Miller, P.R., Wilkins, S.W. (2002). *J. Microsc.* **206**, 33-40.

Schindelin, J., Arganda-Carreras, I., Frise, E., Verena Kaynig, Longair, M., Pietzsch, T., Preibisch, S., Rueden, C., Saalfeld, S., Schmid, B., Tinevez, J.Y., White, D.J., Hartenstein,V., Eliceiri, K., Tomancak, P., Cardona, A. (2012). *Nature Methods* **9**, 676-682.